Modeling the dielectric response of atomistic and continuous media with the split-charge method

Martin H. Müser

Jülich Supercomputing Centre, Institute for Advanced Simulation,
Research Centre Jülich, 52425 Jülich, Germany
E-mail: m.mueser@fz-juelich.de

Many processes involving ions, polar molecules, or polar moieties take place in an external medium with heterogeneous dielectric properties. Examples range from protein folding in a polarizable solvent to contact electrification induced by the rubbing of two dislike solids. When simulating such processes, it is not appropriate to decompose the electrostatic forces between the central atomistic degrees of freedom into (effective) two-body contributions. Instead, one needs to consider the dielectric response of the external medium, which one may want to represent as a continuum. In this contribution, we show that the split-charge equilibration (SQE) method can be used to describe continua with well-defined dielectric properties, although it was originally designed to assign atomic charges on the fly. As such, SQE bears much potential for hybrid particle-continuum simulations. The comparison of dielectric response functions as obtained by SQE and point dipole methods reveals many advantages for SQE. The main points are: SQE requires fewer floating point operations, non-local dielectric properties are more easily embedded, and the leading-order corrections to the continuum limit are isotropic on the simple cubic lattice in contrast to point dipole models.

1 Introduction

The electrostatic polarization of an embedding medium can strongly affect the interaction between ions, polar molecules, or other polar degrees of freedom. To illustrate this point, consider an anion with elementary charge close to a surface of a highly polarizable medium, such as water or, in the extreme case, a metal. If we neglect the surface dipole of the polarizable medium and the induced dielectric response, no (long-range) interaction takes place. However, assuming an ideal mirror charge, the anion feels a Coulomb attraction $V = -e^2/4\pi\varepsilon_0 d$, where d is the distance between the anion and its mirror image. The numerical value of the correction to a non-polarizable treatment for $d = 10$ Å amounts to as much as $V \approx 1.44$ eV, which is roughly 55 times the thermal energy k_BT at room temperature. This number distinctly exceeds the typical energy difference of ten times k_BT between the ground state energy of a folded protein and the first meta-stable conformation.

If the ion is part of a fluid or a solid, that is, if it is part of the central zone of interest, the "effective self-interaction" that the ion experiences from the external medium is not quite as strong as if the ion is in isolation. This is because condensed matter tends to arrange such that it avoids local electrostatic monopoles. The ion then experiences not only its own induced mirror charge but also that of a nearby charge-balancing counterion. As an example, an ideal point dipole of 1.85 D (the value for an isolated water molecule) must be as close as 5.5 Å to its mirror dipole to acquire an effective self-interaction energy of roughly k_BT. Yet, the annihilation of the induced forces may not be sufficiently systematic to make polarization corrections negligible, because polar molecules or moieties can adopt a preferential orientation near interfaces formed by two materials with different dielectric

properties. For this and related reasons, the electric polarization needs to be accounted for in accurate simulations of ionic and polar media[1–4]. Since most systems are heterogeneous and boundary conditions are more complicated than those of semi-infinite metal walls, it is futile to derive effective interactions between the explicitly treated atomistic degrees of freedom. Instead, it is desirable to compute the polarization of the embedding medium, ideally by exploiting continuum descriptions and appropriate meshing far away from the zone of interest.

Often, polarization in condensed matter systems is accounted for by placing inducible (point) dipoles onto atoms or (super) atoms[5–7]. However, in addition to electrostatic polarization of atoms, there can be charge transfer between them. Although there is no *unique* scheme breaking down the polarization into intra- and inter-atomic contributions[8] (mainly because partial atomic charges cannot be defined unambiguously[9]), recent advances show that it is yet both meaningful and practical to do so[10]. We shall not repeat the arguments here and instead simply assume as a heuristic working hypothesis that charge transfer between atoms and the polarization of atoms can be assigned meaningfully.

Determining the set of partial charges $\{Q\}$ and/or atomic dipoles $\{\mu\}$ – plus potentially higher-order multipoles – is usually done using minimization principles[11]. The idea is to find an approximation for the potential energy of the system $V = V(\{Q, \mu ...\})$ by Taylor expanding V with respect to the set of the (small) parameters $\{Q, \mu, ...\}$ and to find well-motivated expressions for the expansion coefficients. In this work, we will base this expansion on the split-charge equilibration (SQE) model[12], in which atomic charges result from the charge transfer through chemical bonds. In addition to fractional charges, atoms can receive integer charges, which, however, are not subjected to bond energy penalties but only to on-site interactions. The SQE method has been recently justified from density-functional theory based arguments[10]. The gist of this justification is that the non-locality of the kinetic energy in DFT (which leads to the shell structure of atoms and to band gaps in solids) can be expressed correctly in leading order by the split-charge terms (which are needed to yield a dielectric response differing from that of metals).

The SQE method was proposed as a unified model of the original chemical-potential-equalization method also known as charge equilibration[13,14] (QE) and the atom-atom charge transfer approach (AACT)[15]. It turns out that SQE avoids the (mutually exclusive) disadvantages of QE and AACT method without introducing new ones. For example, QE automatically produces a metallic response, i.e., a diverging dielectric permittivity, ε_{r}, while AACT can only mimic systems for which $\varepsilon_{\mathrm{r}} - 1 \lesssim 1$ holds[16]. In contrast, SQE can reproduce any arbitrary value of $\varepsilon_{\mathrm{r}} > 1$. In this contribution, we focus on the dielectric properties of SQE and compare them to those produced by approaches in which the dielectric response results from point dipoles.

The remaining part of this chapter is organized as follows: In Section 2, the charge transfer and point dipole models are introduced within one common framework. In Section 3, the continuum limit is derived for a pure SQE model and a pure point dipole model on the simple cubic lattice. Further properties of charge-equilibration methods, that is, those pertaining to molecular systems, are summarized in Section 4. Conclusions are drawn in Section 5. In the appendix, Section 6, details on the dipole-dipole interactions are presented.

2 Charge transfer approaches and the split charge model

As mentioned in the introduction to this chapter, the goal is to find an expansion for the energy as a function of the partial charges and the dipoles – plus potentially higher-order electrostatic multipoles – as a function of the atomic coordinates:

$$V(\{\mathbf{R}, Q, \mu\}) = V(\{\mathbf{R}, Q_0, \mu_0\}) + \sum_i \left\{ \frac{\partial V}{\partial Q_i} \Delta Q_i + \frac{\partial V}{\partial \mu_{i\alpha}} \Delta \mu_{i\alpha} \right\}$$
$$+ \sum_{i,j} \left\{ \frac{1}{2} \frac{\partial^2 V}{\partial Q_i \partial Q_j} \Delta Q_i \Delta Q_j + \frac{\partial^2 V}{\partial Q_i \partial \mu_{j\alpha}} \Delta Q_i \Delta \mu_{j\alpha} + \frac{1}{2} \frac{\partial^2 V}{\partial \mu_{i\alpha} \partial \mu_{j\beta}} \Delta \mu_{i\alpha} \Delta \mu_{j\beta} \right\} \quad (1)$$

We truncate after second order and after the dipole terms. Here, $\{Q_0\}$ and $\{\mu_0\}$ denote, respectively, a set of reference values for atomic charges and dipoles. In the following, we will assume that these can be set to zero unless mentioned otherwise. Moreover, Roman indices refer to atom numbers while Greek indices enumerate Cartesian coordinates, e.g., $\mu_{i\alpha} \equiv \mu_{i\alpha 0} + \Delta\mu_{i\alpha}$ is the α component of the dipole on (super)atom i. For Cartesian indices, we use the summation convention. Some terms in the Taylor expansion Eq. (1) can be readily interpreted.

For isolated atoms, $\partial V/\partial Q_i$ corresponds to the electronegativity χ_i (plus potentially a coupling to an external electrostatic potential), while $\partial^2 V/\partial Q_i^2$ can be associated with the chemical hardness κ_i. They can be parameterized via finite-difference approximations of the ionization energy I_i and electron affinity A_i. The latter two quantities can be be obtained by removing or adding an elementary charge e from atom i,

$$I_i = \frac{\kappa_i}{2} e^2 + \chi_i e \quad (2)$$

$$A_i = \frac{\kappa_i}{2} e^2 - \chi_i e \quad (3)$$

and thus $\kappa_i = (I_i + A_i)/e^2$ and $\chi_i = (I_i - A_i)/2e$. (These quantities are commonly stated in units of eV, which means that the underlying unit system uses the elementary charge as the unit of charge.) In principle, κ_i and χ_i should depend on the environment, but within a reasonable approximation, they can be taken from values measured for isolated atoms. In practical applications, i.e., when allowing κ_i and χ_i to be free fit parameters, they turn out within $\mathcal{O}(10\%)$ of their experimentally determined values[12,17]. Furthermore, it is tempting to associate the mixed derivative $\partial^2 V/\partial Q_i \partial Q_j$ ($i \neq j$) with the Coulomb potential, at least if $\mathbf{R}_i$ and $\mathbf{R}_j$ are sufficiently distant. For nearby atoms, one may want to screen the Coulomb interaction at short distance to account for orbital overlap.

All terms related to the atomic dipoles can be interpreted in a straightforward fashion. The negative of $\partial V/\partial \mu_{i\alpha}$ is the α component of the electrostatic field at $\mathbf{R}_i$ due to external charges. The single-atom terms $\partial^2 V/\partial \mu_{i\alpha} \partial \mu_{i\beta}$, can be associated with the inverse polarizability $1/\gamma_i$ of atom i. Unlike for the charges, practical applications find a large dependence of the polarizability on the chemical environment (in particular for anions)[18], including a direction dependence for directed bonds. The two-atom terms $\partial^2 V/\partial Q_i \partial \mu_{j\alpha}$ and $\partial^2 V/\partial \mu_{i\alpha} \partial \mu_{j\beta}$ correspond to the charge-dipole and dipole-dipole Coulomb interaction, respectively, at least for large distances R_{ij} between atoms i and j.

Unfortunately, it is incorrect to assume that the second-order derivatives $\partial V^2/\partial Q_i \partial Q_j$ quickly approach the Coulomb interaction as R_{ij} increases beyond typical atomic spacings, which one might conclude from the argument that chemistry is local. This can be

seen as follows: we know that isolated fragments (such as atoms or molecules) take integer charges, in many cases zero charge. If we separate two atoms, such as sodium and chlorine to large separation, we would find that the fragments carry a fractional charge

$$Q_{\mathrm{Na,Cl}} = \pm \frac{\chi_{\mathrm{Cl}} - \chi_{\mathrm{Na}}}{\kappa_{\mathrm{Na}} + \kappa_{\mathrm{Cl}} - 1/(4\pi\varepsilon_0 R_{\mathrm{NaCl}})}, \tag{4}$$

assuming that $\partial V^2/\partial Q_i \partial Q_j$ quickly approaches the Coulomb potential. Using element-specific numerical values[19], one obtains partial charges of $\pm 0.4\ e$ for a completely dissociated dimer. However, both atoms should be neutral, because $I_{\mathrm{Na}} > A_{\mathrm{Cl}}$, which requires one to prevent non-local (fractional) charge transfer.

What needs to be done is to penalize the transfer of (fractional) charge over long distances, i.e., when the overlap of orbitals of isolated atoms or ions ceases to be of importance. This can be done as follows. We write the charge of an atom as[12,16]

$$Q_i = n_i e + \sum_j q_{ij}, \tag{5}$$

where n_i is called the oxidation state of the atom and q_{ij} is the charge donated from atom j to atom i, which is called the split charge. By definition, $q_{ij} = -q_{ji}$. (One may object that such an assignment is meaningless as electrons are indistinguishable. However, assignments can be made unique, e.g., by defining an appropriate Penrose inverse for the reconstruction of split charges from charges[10].) Next, we do not only penalize built-up of charge on atoms but also the transfer of charge. Thus, the terms in Eq. (1) exclusively related to partial atomic charges become

$$\begin{aligned} V(\{\mathbf{R}, Q, \cdots\}) = &\sum_i \left\{ \frac{\kappa_i}{2} Q_i^2 + (\chi_i + \Phi_i^{\mathrm{ext}}) Q_i \right\} \\ &+ \sum_{i,j>i} \left\{ \frac{\kappa_{ij}}{2} q_{ij}^2 + \frac{S_{ij}(R_{ij})}{4\pi\varepsilon_0 R_{ij}} Q_i Q_j \right\} + \mathcal{O}(\mu). \end{aligned} \tag{6}$$

Here, we have introduced the split-charge or bond hardness κ_{ij}, which is generally distance and also environment dependent, i.e., it diverges as R_{ij} becomes large, prohibiting the transfer of charge over long distances. Moreover, $S_{ij}(R_{ij})$ denotes a screening at small distances with $S_{ij}(R_{ij}) \to 1$ for $R_{ij} \to \infty$.

Eq. (6) represents the SQE model. The original QE arises in the limit of vanishing bond hardness term κ_{ij}, while the AACT model neglects the atomic-hardness terms κ_i. Partial charges of atoms are deduced by minimizing the energy with respect to the split charges q_{ij}. The total charge of the system automatically adjusts to $Q_{\mathrm{tot}} = \sum_i n_i e$ owing to the $q_{ij} = -q_{ji}$ symmetry. The minimization of V with respect to the split charges can be done with the usual strategies for finding minima of second-order polynomials, such as steepest descent (good and easy for systems with large band gap, i.e., large values of κ_{s}, reasonable convergence in two or three iterations), extended Lagrangians (not efficient for systems with zero or small band gap), or conjugate gradient (probably best when dealing with small or zero band gap systems). Matrix inversion of the Hessian matrix is strongly disadvised due to unfavorable scaling with particle number. Once the partial charges are determined, forces arising due to electrostatic interactions can be computed from $\partial V(\{\mathbf{R}, Q, \cdots\})/\partial R_{i\alpha}$.

The numerical overhead of SQE versus QE is minimal, if present at all. As a matter of fact, since QE models all materials as metallic (as we shall see later), SQE requires much fewer iterations to convergence than QE, at least for systems with a band gap. However, there is a memory overhead within the SQE formulation. For example, assuming 12 neighbors per atom on average, one obtains six split charges per atom, which need to be stored in memory. Despite of this memory overhead in SQE, the number of floating-point operations per SQE minimization step is not much larger than for QE. The reason is that the bulk of the calculations is related to the evaluation of the Coulomb potential $V_{\rm C}$ and the derivatives $\partial V_{\rm C}/\partial Q_i$. Once the latter are known and stored in arrays, the derivatives $\partial V_{\rm C}/\partial q_{ij}$ can be obtained with little CPU time via

$$\frac{\partial V_{\rm C}}{\partial q_{ij}} = \frac{\partial V_{\rm C}}{\partial Q_i} - \frac{\partial V_{\rm C}}{\partial Q_j}, \tag{7}$$

since $dQ_k/dq_{ij} = \delta_{ik} - \delta_{jk}$.

3 The continuum limit of charge equilibration models

In this section, the (static) dielectric response function of the SQE model (augmented with inducible point dipoles) is explored in the continuum limit. Such a treatment contains the original QE and the AACT model as limiting cases. The presentation here explores a similar model discussed previously[20], i.e., a simple cubic crystal in which a "slowly" varying electrostatic field $\mathbf{E}^{\rm ext}(\mathbf{R})$ produced by "external" charges is added. [a] The derivation of the dielectric permittivity pursued is simplified with respect to the original one and moreover, we no longer restrict ourselves to the capacitor geometry.

The charge $Q(\mathbf{R})$ at lattice site $\mathbf{R}/a = l\mathbf{e}_x + m\mathbf{e}_y + n\mathbf{e}_z$ (a being lattice constant) can be calculated through the following second-order, finite-difference approximation to

$$Q(\mathbf{R}) = -\sum_{\Delta\mathbf{R}} \Delta\mathbf{R}\cdot\nabla q(\mathbf{R},\Delta\mathbf{R}), \tag{8}$$

where $\Delta\mathbf{R}$ is a lattice vector. For $\Delta\mathbf{R}$ being a nearest-neighbor vector, the split-charge field $q(\mathbf{R},\Delta\mathbf{R})$ shall be interpreted as follows: $q([x+a/2,y,z],a\mathbf{e}_1)$ is the split-charge donated from the atom located at (x,y,z) to that at $(x+a,y,z)$. (This way, the expression $\Delta\mathbf{R}\,q(\mathbf{R},\Delta\mathbf{R})$ can be seen as a dipole centered at $\mathbf{R}+\Delta\mathbf{R}/2$.) Because similar relations hold for split charges shared between next-nearest atoms, etc., the summation in Eq. (8) can be generalized to any lattice vector $\Delta\mathbf{R}$. To clarify Eq. (8), we note that the split-charge field on the r.h.s. is a function defined on a continuous variable $\mathbf{R}$. The field is chosen such that it is as smooth as possible but nevertheless represents exactly the true split charge exchanged between nearest (or farther) neighbors at the center of the (imaginary) bond of the two atoms exchanging a split charge. The l.h.s. of Eq. (8) is a discrete charge at lattice site $\mathbf{R}$. By dividing $Q(\mathbf{R})$ through a^3, it can be turned into a continuous charge density.

[a] It is probably more meaningful to refer to a continuous-background charge distribution that is not treated explicitly rather than to an external charge distribution. Moreover, the term "slowly varying" shall imply that the charge distribution is continuous, e.g., it only lives on one single wavelength within the first Brillouin zone of the crystal.

In reciprocal space, Eq. (8) becomes

$$\tilde{Q}(\mathbf{k}) = -i \sum_{\Delta\mathbf{R}} \mathbf{k} \cdot \Delta\mathbf{R}\ \tilde{q}(\mathbf{k}, \Delta\mathbf{R}). \tag{9}$$

A difficulty that arises when exchanging split charges with next-nearest neighbors is that we need additional split charge fields, i.e., those living on lattice sites for which $l+m+n$ is odd and those for which $l+m+n$ is even. This means that our simple cubic lattice needs to be subdivided into two interpenetrating face-centered cubic lattices, which makes the analytical discussion intransparent. The need for different lattices will disappear for external fields that have a wavelength much exceeding a lattice constant. It is only in this latter case that the conversion from a discrete theory to a continuum theory as initiated in Eq. (9) is meaningful. Short wavelengths would have to be treated differently. At this point, it shall suffice to state that it is possible, in principle, to tune the next-nearest neighbor bond hardness independently from that of nearest neighbors. This would mean that the polarizability at a wavelength $2a$ can be set independently from that at wavelength a. Similar comments apply when including third-nearest neighbors, etc. Therefore, it should be possible to design a dielectric permittivity such that it reproduces a desired wavelength dependence. For reasons of clarity, we keep Eq. (9) without introducing independent split charges fields living on different sublattices. (Of course, an alternative approach to increasing the unit cell would be to couple different $\mathbf{k}$ vectors defined for the original unit cell.)

Including point dipoles to the lattice sites, the split-charge energy for a perfect (monoatomic, $\chi \equiv 0$) lattice reads

$$\begin{aligned} V = & \sum_{\mathbf{R}} \left\{ \frac{\kappa}{2}\, Q^2(\mathbf{R}) + \sum_{\Delta\mathbf{R}} \frac{\kappa_{\mathrm{s}}(\Delta\mathbf{R})}{2}\, q^2(\mathbf{R}, \Delta\mathbf{R}) - \mathbf{E}^{\mathrm{ext}}(\mathbf{R}) \cdot \Delta\mathbf{R}\ \nabla q(\mathbf{R}, \Delta\mathbf{R}) \right\} \\ & + \sum_{\mathbf{R}} \left\{ \frac{1}{2\gamma} \mu_\alpha^2(\mathbf{R}) - E_\alpha^{\mathrm{ext}}(\mathbf{R}) \mu_\alpha(\mathbf{R}) \right\} + \sum_{\mathbf{R},\mathbf{R}'} \left\{ \frac{J(\Delta\mathbf{R})}{2} Q(\mathbf{R}) Q(\mathbf{R}') \right. \\ & \left. + J_\alpha(\Delta\mathbf{R}) Q(\mathbf{R}) \mu_\alpha(\mathbf{R}') + \frac{J_{\alpha\beta}(\Delta\mathbf{R})}{2} \mu_\alpha(\mathbf{R}) \mu_\beta(\mathbf{R}') \right\}. \end{aligned} \tag{10}$$

Here, $J(\Delta\mathbf{R})$ is the (screened) Coulomb interaction between the charges $Q(\mathbf{R})$ and $Q(\mathbf{R}')$, the singly-indexed $J_\alpha(\Delta\mathbf{R})$ represents the (screened) charge-dipole interaction, and the doubly-indexed $J_{\alpha\beta}(\Delta\mathbf{R})$ is the dipole-dipole interaction. Moreover, $\Delta\mathbf{R} \equiv \mathbf{R} - \mathbf{R}'$ and any Coulomb coupling (from monopole-monopole to dipole-dipole interaction) is set to zero for $\Delta\mathbf{R} = 0$.

Eq. (10) is easily transformed into reciprocal space, as only bilinear coupling occurs. To do so, one needs to replace sums over $\mathbf{R}$ with sums over $\mathbf{k}$ and follow the known rules for Fourier transforms, for instance, the atomic hardness term becomes $\sum_{\mathbf{k}} \kappa \tilde{Q}(\mathbf{k}) \tilde{Q}^*(\mathbf{k})/2$. See also the appendix.

The solutions $\tilde{q}(\mathbf{k}, \Delta\mathbf{r})$ minimizing V must satisfy $\partial V / \partial \tilde{q}(\mathbf{k}, \Delta\mathbf{R}) = 0$, which reads

$$\left\{ \kappa + \tilde{J}(\mathbf{k}) \right\} k_\alpha \Delta R_\alpha \tilde{Q}(\mathbf{k}) + \kappa_{\mathrm{s}}(\Delta\mathbf{R}) \tilde{q}(\mathbf{k}, \Delta\mathbf{R}) = \tilde{E}_\alpha^{\mathrm{eff}}(\mathbf{k}) \Delta R_\alpha \tag{11}$$

with

$$\tilde{E}_\alpha^{\mathrm{eff}}(\mathbf{k}) = \tilde{E}_\alpha^{\mathrm{ext}}(\mathbf{k}) - k_\alpha \tilde{J}_\beta(\Delta\mathbf{k}) \tilde{\mu}_\beta(\mathbf{k}). \tag{12}$$

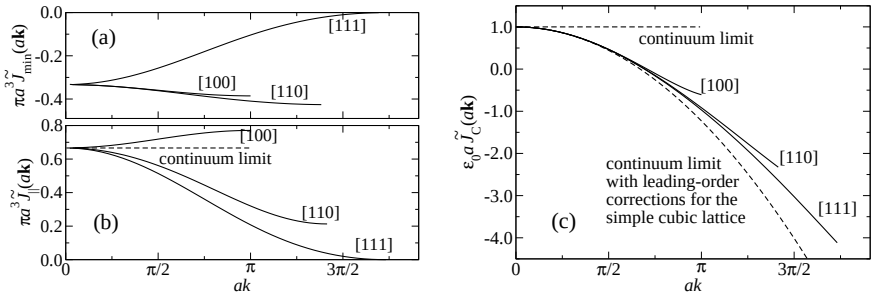

Figure 1. (a) Minimum eigenvalues of the dipole coupling matrix $\tilde{J}_{\alpha\beta}(\mathbf{k})$ for selected paths in the first Brillouin zone of the simple cubic lattice. (b) The coupling of dipoles oriented parallel to the given $\mathbf{k}$ vector as a function of the wavenumber along selected paths. (c) Fourier transform of the Coulomb interaction $\tilde{J}_{\mathrm{C}}(a\mathbf{k})$ for the simple cubic lattice.

In reciprocal space, the minimization condition $\partial V/\partial\mu_i(\mathbf{R}) = 0$ becomes

$$\left\{\frac{\delta_{\alpha\beta}}{\alpha} + \tilde{J}_{\alpha\beta}(\mathbf{k})\right\}\tilde{\mu}_\beta(\mathbf{k}) = \tilde{E}^{\mathrm{ext}}_\alpha(\mathbf{k}) - \tilde{J}_\alpha(\mathbf{k})\tilde{Q}(\mathbf{k}). \tag{13}$$

From the set of coupled equations (11) and (13), one can deduce the dielectric response to an external field. We will discuss these solutions in a separate paper. In this contribution, for reasons of simplicity, we focus on the limit in which the coupling between monopoles and dipoles can be neglected. This allows one to work out the differences between the dielectric response functions that are due to either pure dipole or pure bond polarization.

3.1 Pure dipole polarizability

We start our analysis of the dielectric response by neglecting charge transfer. For reasons of simplicity, we consider a sinusoidal electrostatic field that is aligned parallel to the z-axis of our simple cubic solid, i.e., $\mathbf{E}^{\mathrm{ext}}(\mathbf{r}) = E_3\mathbf{e}_3\exp(ik_3z)$. To this end, we need expressions for the $\tilde{J}_{\alpha\beta}(k_3\mathbf{e}_3)$ elements, see also the appendix. The off-diagonal elements must be zero (for $\mathbf{k}$ parallel to z) for reasons of symmetry. Numerically, we find for unscreened dipole-dipole interactions that the diagonal elements can be represented quite accurately via

$$\tilde{J}_{11}(k_3\mathbf{e}_3) = \tilde{J}_{22}(k_3\mathbf{e}_3) \approx \frac{\delta_{k_30} - 1}{3\varepsilon_0 a^3}\left\{1 + 0.156(5)\sin^2(ak_3/2)\right\} \tag{14}$$

$$\tilde{J}_{33}(k_3\mathbf{e}_3) = -2\tilde{J}_{11}(k_3\mathbf{e}_3), \tag{15}$$

which includes the discontinuous drop from a finite value at $k_3 = 0^+$ to zero at $k = 0$. It is furthermore well known[21] that the dispersion of the $\tilde{J}_{\alpha\beta}(\mathbf{k})$ depends on $\mathbf{k}$. This dependence is sketched along some lines in the first Brillouin zone in Fig. 1(b). One can see that the corrections to the continuum limit depend not only on the magnitude of $\mathbf{k}$ but also on its orientation.

We start our discussion with the analysis of the split charges exchanged in a direction normal to the external field, i.e., in x-direction. According to Eq. (9)

$$\left\{\frac{1}{\gamma} + \tilde{J}_{11}(k_3\mathbf{e}_3)\right\}\tilde{\mu}_1(k_3\mathbf{e}_3) = 0, \tag{16}$$

Using Eq. (14) for $\tilde{J}_{11}(k_3\mathbf{e}_3)$, one can see that the prefactor on the l.h.s. of the equation can become zero at a finite density ρ, which is defined as $\rho = 1/a^3$. This means that the system can acquire a finite polarization without energy penalty, which in turn implies a polarization catastrophe. For small but non-zero k_3, this happens at the same density $\rho = 3\varepsilon_0/\gamma$ at which the Clausius-Mossotti (CM) relation for dipoles (see Eq. (23) for $k_3 \to 0$) indicates a diverging dielectric constant, namely for $\gamma\rho = 3\varepsilon_0$.

The discrete simple cubic solid becomes unstable at an even smaller density, e.g., for dipoles associated with the wavevector $\mathbf{k} = \pi(0,0,1)/a$ and at even smaller densities for $\mathbf{k} = \pi(1,1,0)$, as one can see from Fig. 1a. Specifically, dipoles with the wavevector $(\pi/a)(1,1,0)$ already become unstable at a density of $\rho = \varepsilon_0/0.4259(3)\gamma$ rather than at $3\varepsilon_0/\gamma$ as in CM.

We next analyze the split-charge response parallel to the z axis. Deriving the regular CM relation from the present treatment is not easily possible. The reason is that the sum over dipoles is only conditionally convergent – hence the discontinuity of the $\tilde{J}_{\alpha\beta}(\mathbf{k})$ at the Γ point. Due to the conditional convergence, the shape of the material matters when determining its dielectric response. For the regular capacitance geometry, the static dielectric constant consistent with CM relation requires summing up planes of interacting dipoles, where each plane is normal to the the z axis[22]. Here, we proceed using a different approach, previously pursued to derive the (macroscopic) dielectric response function[23].

What we seek is a relation between the polarization $\mathbf{P} \equiv \langle\mu_\alpha\rangle\mathbf{e}_\alpha/a^3$ and the coarse-grained total electrostatic field $\mathbf{E}^{\mathrm{tot}}$ through the equation

$$\frac{1}{a^3}\tilde{\mu}_\alpha(\mathbf{k}) = \varepsilon_0 \left\{\tilde{\varepsilon}_{\alpha\beta}(\mathbf{k}) - \delta_{\alpha\beta}\right\} \tilde{E}^{\mathrm{tot}}_\beta(\mathbf{k}), \tag{17}$$

where $\tilde{\varepsilon}_{\alpha\beta}(\mathbf{k})$ is the dielectric tensor. So far, we only have a relation between the dipoles and the electrostatic field due to external charges, i.e., for the z-component

$$\left\{\frac{1}{\gamma} + \tilde{J}_{33}(k_3\mathbf{e}_3)\right\} \tilde{\mu}_3(k_3\mathbf{e}_3) = \tilde{E}^{\mathrm{ext}}_3(k_3\mathbf{e}_3). \tag{18}$$

The total field is the superposition of a slowly varying field due to external charges and a rapidly varying field produced by the dipoles. The latter consists of two contributions. One is the field coming from "outside" the dipoles, i.e., the one we used to sum up the dipole-dipole interactions. The other contribution stems from the "internal" field within the point dipole[23]. It can be represented as a δ-function singularity if the dipole is located at the origin, see the appendix:

$$E^{\mathrm{int}}_\alpha(\mathbf{r}) = -\mu_\alpha \frac{\delta(\mathbf{r})}{3\varepsilon_0}. \tag{19}$$

At a given lattice point, we define the coarse-grained field according to

$$E^{\mathrm{tot}}_\alpha(\mathbf{R}) = E^{\mathrm{ext}}_\alpha(\mathbf{R}) + \frac{1}{a^3}\int_{V_{\mathrm{E}}(\mathbf{R})} d^3r \left\{E^{\mathrm{dip}}_\alpha(\mathbf{r}) - \frac{\mu_\alpha(\mathbf{R})}{3\varepsilon_0}\right\}, \tag{20}$$

where $V_{\mathrm{E}}(\mathbf{R})$ is a cubic elementary cell of size a^3 with its center of mass located at $\mathbf{R}$. With this choice, the dipole field from the dipole contained in $V_{\mathrm{E}}(\mathbf{R})$ does not contribute to the coarse-grained field. To leading order, we approximate the value of $E^{\mathrm{dip}}_\alpha(\mathbf{r})$ within

$V_{\mathrm{E}}(\mathbf{R})$ through $E_\alpha^{\mathrm{dip}}(\mathbf{R})$ produced by dipoles from outside of $V_{\mathrm{E}}(\mathbf{R})$. This makes the $\tilde{J}_{33}(k_3\mathbf{e}_3)$ term on the r.h.s. of Eq. (18) disappear and thus

$$\left\{\frac{1}{\alpha}-\frac{1}{3\varepsilon_0 a^3}\right\}\tilde{\mu}_3(k_3\mathbf{e}_3)\approx\tilde{E}_3^{\mathrm{tot}}(k_3\mathbf{e}_3). \tag{21}$$

At this level of approximation, i.e., for $\langle E_\alpha^{\mathrm{dip}}(\mathbf{r})\rangle_{V_{\mathrm{E}}(\mathbf{R})}\approx E_\alpha^{\mathrm{dip}}(\mathbf{R})$, the response function is dispersion-free and moreover continuous at the Γ point. However, each mode becomes unstable at the same value of k_3. This contradicts our previous result (exact for point dipoles) for the polarization catastrophe in x direction, which – for simple cubic – is symmetry related to that in z. The problem can be fixed by re expressing Eq. (21) as

$$\varepsilon_0 a^3\left\{\frac{1}{\gamma}-\frac{\delta_{k_30}}{3\varepsilon_0 a^3}-\frac{J_{33}(k_3\mathbf{e}_3)}{2}\right\}\frac{\tilde{\mu}_3(k_3\mathbf{e}_3)}{a^3}=\varepsilon_0\tilde{E}_3^{\mathrm{tot}}(k_3\mathbf{e}_3), \tag{22}$$

where we have introduced some factors to simplify the comparison to Eq. (17). Such a comparison yields

$$\begin{aligned}\tilde{\varepsilon}_{33}(k_3\mathbf{e}_3)-1&=\frac{\gamma/\varepsilon_0 a^3}{1-\gamma\delta_{k_30}/3\varepsilon_0 a^3-\gamma\tilde{J}_{33}(k_3\mathbf{e}_3)/2}\\&=\frac{\gamma/\varepsilon_0 a^3}{1-\gamma/3\varepsilon_0 a^3\left\{1+0.156(5)\sin^2(ak_3/2)\right\}}\end{aligned} \tag{23}$$

The last two relations state that the dielectric tensor element $\tilde{J}_{33}(k_3\mathbf{e}_3)$ is continuous at the Γ point. Furthermore, Eq. (23) is equivalent to the CM relation at $k_3=0$ and $k_3\to 0$.

The treatment parallel to other (symmetry) directions is similar to the one presented so far. However, it becomes more complicated when $\mathbf{k}$ does not lie on a symmetry line, because the eigenvectors of the coupling matrix are no longer purely parallel or orthogonal to $\mathbf{k}$. This means that the polarization induced in the crystal is no longer parallel to the (static) electrostatic field induced by the external charge distribution. Thus, the dielectric response functions quickly deviates from being isotropic with increasing wavenumber.

3.2 Pure charge transfer polarizability

As argued before, one of the promising properties of the SQE model is that one can define non-local charge transfer resulting in non-local response functions. However, there are quite a few differences between point-dipole polarizability and split-charge polarizability at a level where we only allow for charge transfer between adjacent atoms on the simple cubic lattice.

To keep the formalism transparent, we will first restrict split charges to nearest neighbors. [b] In analogy to our previous treatment[20], we write nearest-neighbor split charges as a vector $q_\alpha(\mathbf{R})$, where $q_1(\mathbf{R}+a\mathbf{e}_1/2)$ is the split charge donated from the atom located at $\mathbf{R}$ to the one at $\mathbf{R}+a\mathbf{e}_1$. This allows one to rewrite Eq. (9) as

$$\tilde{Q}(\mathbf{k})=-ik_\alpha\tilde{q}_\alpha(\mathbf{k}). \tag{24}$$

[b] When describing non-local charge transfer on the continuum scale through Eq. (9), one can proceed as done in the current text. One only needs to divide Eq. (11) by $\kappa_{\mathrm{s}}(\Delta\mathbf{R})$, multiply the equation with the wavenumber and sum it over all $\Delta\mathbf{R}$. This way, one obtains an equation for $\tilde{Q}(\mathbf{k})$ with effective values for the split-charge hardness and the Coulomb interaction.

Assuming the same sinusoidal electrostatic field parallel to the z axis as in the previous section and no point dipoles on atoms, Eq. (11) can be written as

$$\left[\left\{\kappa + \tilde{J}(k_3\mathbf{e}_3)\right\}(ak_3)^2 + \kappa_\mathrm{s}\right]\tilde{q}_3(k_3\mathbf{e}_3) = a\tilde{E}_3^\mathrm{ext}(k\mathbf{e}_3). \tag{25}$$

To derive the expression for the dielectric permittivity, we proceed similarly as in the previous section, rather than as in the original literature[20]. First we identify $aq_3(\mathbf{R})$ as the dipole per volume $V_\mathrm{E} = a^3$ and thus $P_3(\mathbf{R}) = q_3(\mathbf{R})/a^2$ is the local polarization. Next we convert from an external electrostatic field to a total, coarse-grained field on the r.h.s. of the equation by eliminating the Coulomb interaction on its l.h.s. The difference to the previous section is that we do not need to take care of internal dipole fields, because the Coulomb interactions are solely related to point charges. Thus,

$$a\varepsilon_0\left\{\kappa(ak_3^2) + \kappa_\mathrm{s}\right\}\frac{\tilde{q}(k_3\mathbf{e}_3)}{a^2} = \varepsilon_0\tilde{E}_3^\mathrm{tot}(k\mathbf{e}_3). \tag{26}$$

Comparison with Eq. (17) yields

$$\tilde{\varepsilon}_{33}(k_3\mathbf{e}_3) - 1 = \frac{1}{\varepsilon_0 a\{\kappa_\mathrm{s} + \kappa(ak_3)^2\}}, \tag{27}$$

which is equivalent to Eq. (27) in Ref. 16 but contains in addition a dispersion correction due to atomic hardness. Here, we note that we used simple finite-difference approximations to deduce the charges from the split-charge field. This is why $\tilde{\varepsilon}_{33}(\mathbf{k})$ does not turn out periodic in the Brillouin zone. The problem can be easily fixed without changing the leading-order behavior of the dielectric susceptibility by replacing Eq. (27) with

$$\tilde{\varepsilon}_{33}(k_3\mathbf{e}_3) - 1 = \frac{1}{\varepsilon_0 a\{\kappa_\mathrm{s} + 4\kappa\sin^2(ak_3/2)\}}, \tag{28}$$

which is equivalent to replacing Eq. (24) with the accurate relation $\tilde{Q} = \sum_{\Delta\mathbf{R}}\{\exp(-i\mathbf{k}\cdot\Delta\mathbf{R}) - 1\}\,\tilde{q}(\mathbf{k}, \Delta\mathbf{R})$.

Formally, Eq. (28) expresses a similar functional dependence of $\tilde{\varepsilon}_{33}(k_3\mathbf{e}_3)$ on k_3 as that derived for pure dipole polarization, see Eq. (23). However, there are differences between them in practice. First, the leading continuum corrections for small but finite k are isotropic for the SQE model but not for the point dipole model. Second, the prefactor to the corrections is small for dipoles, i.e., of order 0.1. Conversely, the ratio κ/κ_s tends to be of order unity or much greater. This is because $\kappa_\mathrm{s}e^2$ can be associated with the band gap of solids[16] (in fact, κ_s is an upper bound for the band gap), so that κ_s (for true chemical bonds) can be anything between zero and values a few times the atomic hardness. Next, the dielectric response in the SQE formalism does not automatically diverge at high density for fixed dipole or bond polarizability. The reason is that the total Hessian can be made positive definite through the choice of large atomic hardness. This is different from the AACT model, which necessitates small bond polarizability to keep the Hessian positive definite.

Fig. 2 demonstrates that the dielectric permittivity, $\varepsilon_\mathrm{r} = \tilde{\varepsilon}_{33}(0)$, is indeed independent of the atomic hardness. Moreover, one recognize that the dielectric response does indeed not diverge even if κ_s is very small. For the smallest value of the bond hardness ($\kappa_\mathrm{s} = 1/4\varepsilon_0 a$), the point-dipole model with equivalent local polarization ($\gamma = a^2/\kappa_\mathrm{s}$) would have been already beyond the polarization catastrophe, i.e., it would have produced a negative dielectric constant of $\varepsilon_\mathrm{r} = 4/(1 - 4/3) = -12$.

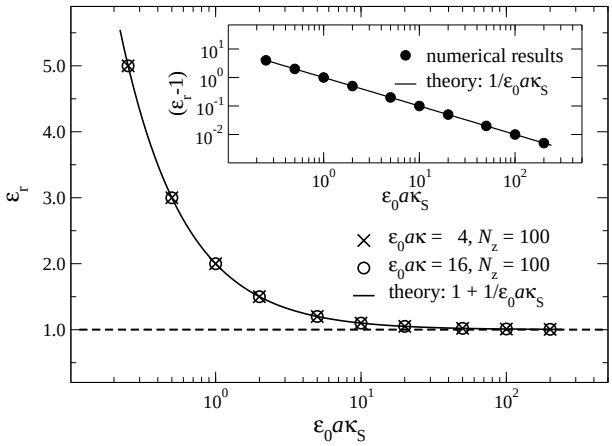

Figure 2. Dielectric permittivity for different choices of κ and $\kappa_{\rm s}$. The numerical results were obtained in a regular capacitor geometry, in which $N_z = 100$ layers containing 10×10 atoms were placed into a simulation cell. Periodic boundary conditions were applied in all three spatial dimensions, however, in the direction of the electrostatic field, a gap was introduced. The dielectric permittivity was obtained by measuring the coarse-grained total electrostatic field within and outside the material. From Ref. 16.

The reason why $\kappa_{\rm s}$ can be made small even at large density is that the atomic hardness impedes large local dipole gradients. Thus, the atomic hardness must introduce some smearing of the response function. To elucidate this claim, we analyze the split-charge response in a capacitor geometry. Thus, we consider an external electrostatic potential that has a constant slope in a periodically repeated cell $\Phi(z) = E_3 z$ but goes back to zero when the periodic image is repeated. The required non-zero Fourier coefficients for the resulting electrostatic field read[16]

$$\tilde{E}_3(k_3\mathbf{e}_3) = -2E_3 \text{ for } k_3 = 2\pi n/L, n \in \mathbb{N}. \tag{29}$$

The associated split charge response is

$$\tilde{q}(k_3) \approx \frac{-2E_0}{\left\{\kappa + \tilde{J}(k_3\mathbf{e}_3)\right\}(ak_3)^2 + \kappa_{\rm s}}, \tag{30}$$

where a reasonable approximation to $\tilde{J}(\mathbf{k})$ was found to be[20]

$$\tilde{J}(\mathbf{k}) = \frac{1 - \nu(ak)^2}{\varepsilon_0 a(ak)^2}. \tag{31}$$

A value of $\nu = 0.22578$ expresses the (isotropic) leading-order discretization corrections for the simple cubic lattice, see Fig. 1. Inserting Eq. (31) into (30) can be written as follows

$$\tilde{q}_{\rm s}(k_3) = \frac{-2E_0}{\kappa'(ak)^2 + \kappa'_{\rm s}} \tag{32}$$

with $\kappa' = \kappa - \nu/\varepsilon_0 a$ and $\kappa'_{\rm s} = \kappa_{\rm s} + 1\varepsilon_0 a$. When solving the response of the dielectric medium, i.e., with the help of the residue theorem, it becomes clear that the roots of the

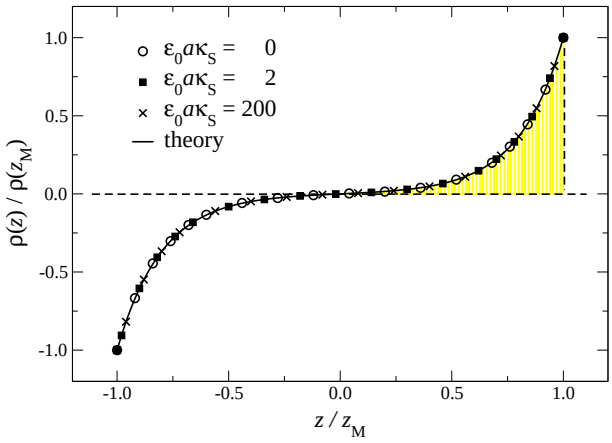

Figure 3. Charge density of a simple cubic SQE model in a constant external electrostatic field as a function of the coordinate z normal to the surface. The bond stiffness varies from metallic to extremely dielectric. The atomic hardness was adjusted such that the penetration depth as defined in Eq. (33) remained constant. The shaded area can be interpreted as total polarization charge. From Ref. 16.

denominator of Eq. (32) have the meaning of an inverse (exponential) decay length δ^{-1}. This can be solved to yield

$$\delta = a\sqrt{\frac{\varepsilon_0 a\kappa - \nu}{1 + \varepsilon_0 a\kappa_\mathrm{s}}}. \tag{33}$$

Thus, the split charge field decays with $q(z) \propto \exp(-|z - z_0|/\delta)$ from the surface located at z_0. The surface polarization charge must obey the same exponential law, because it is proportional to the derivative of $q(z)$. Fig. 3 demonstrates that the expected behavior is borne out in numerical simulations. Their set-up is described in the caption of Fig. 2.

It is instructive to analyze the properties in the limits where either the bond hardness κ_s disappears (as in conventional QE methods) or the atomic hardness κ (as in AACT). First, for $\kappa_\mathrm{s} = 0$ the dielectric constant diverges for small wavevectors according to Eq. (27). This is the behavior of an ideal metal. This result implies that electric field lines are perpendicular to the surface of material modeled within the QE approach. (This is observed in simulations, which shall not be shown here.) Second, for $\kappa = 0$, the dielectric constant is finite. However, a problem that arises is that the Hessian must be positive definite. The smallest value that $\tilde{J}(\mathbf{k})$ takes for unscreened Coulomb interactions on the simple cubic lattice is $-(3\pi^2)M/4\pi\varepsilon_0 a$, where $M = 1.748$ is the Madelung constant of the rock salt lattice. Thus, κ_s must exceed the largest negative eigenvalue of the $\tilde{J}_{\alpha\beta}(\mathbf{k})$ matrix. This is found at $\mathbf{k} = (\pi/a)(1,1,1)$ and the resulting limitation for the the dielectric permittivity is $\varepsilon_\mathrm{r}^\mathrm{AACT} - 1 < 1/1.748$, at least for unscreened Coulomb potentials. This is less than the corresponding value of any condensed matter material. Very small values observed in reality are, for example $\varepsilon_\mathrm{r} \gtrsim 2$ for Teflon or polyethylene. These values are similar to $\varepsilon_\mathrm{r}^\infty(\mathrm{NaCl}) = 2.56$.

4 Further properties of charge equilibration models

Most charge-transfer studies do not focus on periodic systems but are predominantly concerned with molecules. In that context, deficiencies of various models were noted before the analysis presented in the previous section had been conducted. Here, we summarize some of the results on molecular systems.

One of the first problems noted with regular QE is that it does not obey the neutral dissociation limit[24], as can be seen from Eq. (4). The original proposition to fix this problem was to screen chemical potential differences as a function of distance[24]. Unfortunately, this fix is hardly justified in reality and its implementation actually leads to artifacts, e.g., batteries could not work if the chemical potentials between atoms were screened as a function of distance. Screening is only meaningful for electrostatic field lines when there is a medium whose influence is not considered explicitly. But even if field lines were screened, this does not mean that energy differences would be completely damped out. The line integral from one point to another would still remain finite owing to near-field contributions. Moreover, how can screening be justified for a dimer placed in vacuum?

Approaches in which the concept of bond hardness is introduced can be easily parameterized to yield dissociation limits in which the atoms are neutral[12,25] – or have non-zero integer charge[16,26]. All that needs to be done is to make the bond hardness diverge when two atoms or two molecular fragments are moved to large separation. In fact, a quantitative analysis revealed that making the bond stiffness between two atoms simply a function of the distances between the two atoms (without including an environment dependence) already lead to reasonably accurate partial atomic charges of the reactants (initially and near the transition state) and of the products of the bond breaking[25].

It had also been observed that the polarizability of polymers $\gamma(N)$ (e.g. simple alkanes) as treated with QE growths with the third power of the degree of polymerization N in the limit of large N. The correct scaling is linear[27,17]. Some representative results are shown in Fig. 4 and compared to quantum chemical calculations. One can see that the QE model systematically overestimates polarizabilities while SQE shows the correct trend. The SQE data only tends to lie slightly below the quantum chemical results, which is easily explained because the employed SQE model did not allow for atom polarizability. Lastly, QE models ignoring the bond hardness term produce alcohols whose dipole moment increases as the fatty tail of the molecule is made longer, while the dipole quickly levels off at a realistic value within an SQE type treatment[28].

The AACT models do not suffer from the shortcomings of pure QE models. However, they have different deficiencies. For example, they barely show any dispersion of the alkene polarizability $\gamma(N)$ at small N in contrast to the real behavior and that exhibited by SQE models[27]. This behavior can be rationalized from the small (zero) penetration depth δ derived for solids in the last section. Moreover, the AACT model produces negative (chemical) hardnesses of molecules when excess charge is added to a molecule[16].

In conclusion, neither pure bond nor conventional QE model produce the correct constitutive equations, while their combination in form of SQE can be parameterized to reproduce meaningful numbers. In fact, even absolute numbers turn out reasonable[12], e.g., partial charges deduced from SQE were within $\mathcal{O}(10\%)$ accuracy as compared to DFT-based results while QE and AACT deviated by $\mathcal{O}(30\%)$. A comprehensive comparison between SQE and QE also found that SQE clearly outperformed the original QE in all 23

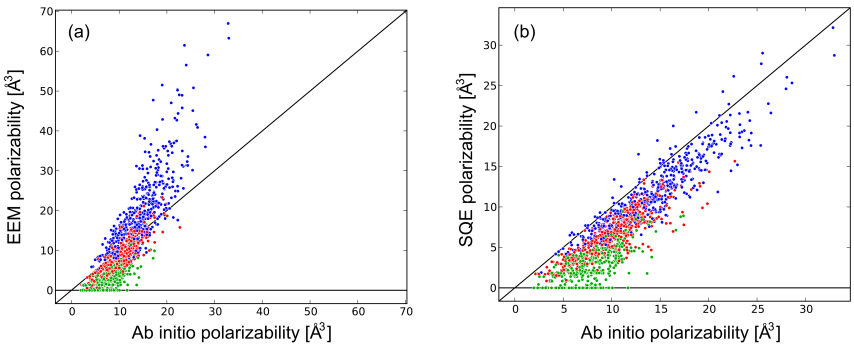

Figure 4. Polarizability of (a) QE and (b) SQE as a function of the polarizability deduced from quantum mechanical calculations on a variety of molecules. Green, red, and blue data points reflect the smallest, the medium, and the largest eigenvalue of the polarizability tensor for different molecules (including varying conformations). From Ref. 17.

benchmark tests on a set of more than 500 organic molecules[17].

The true advantage of SQE, when applied at a molecular level, might yet be a different one: It allows one to introduce formal oxidation states and to treat meaningfully excess integer charge in molecular systems[16,26]. This makes it possible to reproduce the generic features of contact electrification as well as the discharge of batteries, which will be shown in future work.

5 Concluding Remarks

The main part of this contribution is the analysis of the dielectric permittivity as produced by the regular split-charge equilibration model and a model in which point dipoles are placed on discrete lattice sites. While both methods have similar low-density, long-wavelength response functions, there are quite a few differences between them. First, the SQE model is based on summing up (eventually screened) Coulomb interactions between point charges while the point dipole models are based on dipole-dipole interactions. Since the resulting sums are conditionally convergent in both cases, neither one can be cut off at a finite distance without uncontrollable errors. The advantage of the SQE model is that fewer floating point operations are required to evaluate pair interactions, since the coupling of point charges is described by a scalar rather than by a tensor of rank two as for dipoles. Moreover, fast summation methods for Coulomb interactions are readily available. Second, the SQE model produces response functions on the (easy-to-code) simple cubic lattice that are isotropic not only in the continuum limit but also with respect to their leading-order continuum corrections, which are of order k^2. Point dipole models on the simple cubic lattice have direction-dependent k^2 interactions.

A potentially useful advantage of SQE over point-dipole models is that the SQE model can reflect non-local dielectric response functions. This can be done, in principle, by introducing non-local charge-transfer variables. This ability makes the SQE model a promising candidate as a coarse-grained model for water, which is known to have a strong wave-

length dependent dielectric constant[29]. Another advantage of the SQE model is that it is isomorphic to elastic models. The split charges can be treated in analogy to (elastic) displacements in the solid. Thus, coarse-graining of the region and adaptive mashing of SQE can be done in analogy to elastic models.

Acknowledgments

The author thanks W. Dapp and J. Jalkanen for useful discussions.

References

1. A. Warshel and M. Levitt. *J. Mol. Biol.*, 103:227–249, 1976.
2. B. Honig and A. Nicholls. *Science*, 268:1144–1149, 1995.
3. P. Jungwirth and D. J. Tobias. *Chem. Rev.*, 106:1259–1281, 2006.
4. A. Warshel, P. K. Sharma, M. Kato, and W. W. Parson. *Biochim. Biophys. Acta*, 1764:1647–1676, 2006.
5. J. Applequist, J. R. Carl, and K.-K. Fung. *J. Am. Chem. Soc.*, 94:2952, 1972.
6. B. Thole. *Chem. Phys.*, 59:341, 1981.
7. A. Papazyan and A. Warshel. *J. Phys. Chem. B*, 101:11254–11264, 1997.
8. K. G. Denbikh. *Trans. Faraday Soc.*, 36:936–948, 1940.
9. J. Meister and W. H. E. Schwarz. *J. Phys. Chem.*, 98:8245–8252, 1994.
10. T. Verstraelen, P. W. Ayers, V. Van Speybroeck, and M. Waroquier. (submitted to J. Chem. Phys.).
11. S. W. Rick and S. J. Stuart. *Rev. Comp. Chem.*, 18:89, 2002.
12. R. A. Nistor, J. G. Polihronov, M. H. Müser, and N. J. Mosey. *Journal of Chemical Physics*, 125:094108, 2006.
13. R. P. Iczkowski and J. L. Margrave. *J. Am. Chem. Soc.*, 83:3547–3551, 1961.
14. W. J. Mortier, K. van Genechten, and J. Gasteiger. *J. Am. Chem. Soc.*, 107:829, 1985.
15. R Chelli, P Procacci, R Righini, and S Califano. *J. Chem. Phys.*, 111(18):8569–8575, 1999.
16. M. H. Müser. *European Physical Journal B*, 85:135, 2012.
17. T. Verstraelen, V. Van Speybroeck, and M. Waroquier. *J. Chem. Phys.*, 131:044127, 2009.
18. P. W. Fowler and P. A. Madden. *J. Phys. Rev. B*, 29:1035–1042, 1984.
19. J. Robles and L.J. Bartolotti. *J. Am. Chem. Soc.*, 106:3723–3727, 1984.
20. R. A. Nistor and M. H. Müser. *Phys. Rev. B*, 79:104303, 2009.
21. M. H. Cohen and F. Keffer. *Phys. Rev.*, 99:1128–1134, 1955.
22. B. R. A. Nijboer and F. W. De Wette. *Physica*, 6:422–431, 1958.
23. J. H. Hannay. *Eur. Phys. J.*, 4:141–143, 1983.
24. J. Morales and T. J. Martinez. *J. Phys. Chem. A*, 105:2842, 2001.
25. D. Mathieu. *J. Chem. Phys.*, 127:224103, 2007.
26. W. Dapp and M. H. Müser. (in preparation).
27. G. L. Warren, J. E. Davis, and S. Patel. *J. Chem. Phys.*, 128:144110, 2008.
28. P. T. Mikulski, M. T. Knippenberg, and J. A. Harrison. *J. Chem. Phys.*, 131:241105, 2009.

29. P. A. Bopp, A. A. Kornyshev, and G. Sutmann. *Phys. Rev. Lett.*, 76:1280–1283, 1996.

6 Appendix: Dipole-dipole interactions in real and reciprocal space

The field of a dipole μ centered at the origin can be represented according to

$$\begin{aligned}\mathbf{E}(\mathbf{r}) &= \frac{1}{4\pi\epsilon_0}\nabla\left(\mu\cdot\nabla\frac{1}{r}\right)\\ &= \frac{1}{4\pi\epsilon_0}\left(\frac{3(\mu\cdot\mathbf{r})\mathbf{r}-\mu r^2}{r^5}\right)-\frac{\mu}{3\epsilon}\delta(\mathbf{r})\end{aligned} \tag{34}$$

Thus, the potential energy V gained when a second dipole is placed at $\mathbf{r}\neq 0$ reads in tensor notation

$$V = J_{\alpha\beta}(\mathbf{r})\mu_{1\alpha}\mu_{2\beta} \tag{35}$$

with

$$J_{\alpha\beta}(\mathbf{r}) = \frac{-1}{4\pi\epsilon_0}\frac{3r_\alpha r_\beta - r^2\delta_{\alpha\beta}}{r^5}. \tag{36}$$

If dipoles are placed onto a Bravais lattice, such as the simple cubic lattice, it is readily shown – using the properties of the Fourier transform – that the net potential energy

$$V = \frac{1}{2}\sum_{i,j\neq i} J_{\alpha\beta}(\mathbf{R}_i-\mathbf{R}_j)\mu_\alpha(\mathbf{R}_i)\mu_\beta(\mathbf{R}_j) \tag{37}$$

can be expressed in reciprocal space as

$$V = \frac{1}{2}\sum_{\mathbf{k}} \tilde{J}_{\alpha\beta}(\mathbf{k})\tilde{\mu}_\alpha(\mathbf{k})\tilde{\mu}^*_\beta(\mathbf{k}), \tag{38}$$

where $\mathbf{k}$ is a reciprocal lattice vector. Moreover

$$\tilde{J}_{\alpha\beta}(\mathbf{k}) = \sum_{\mathbf{R}\neq 0}\frac{-1}{4\pi\epsilon_0}\frac{3R_\alpha R_\beta - R^2\delta_{\alpha\beta}}{R^5}\exp(-i\mathbf{k}\cdot\mathbf{R}), \tag{39}$$

where the summation runs over all lattice vectors $\mathbf{R}$.

Similar comments apply to the point-point and point-dipole interactions.